




Robust Quasi-Adaptive Beamforming Against Direction-of-Arrival Mismatch

XUEJING ZHANG ¹, Student Member, IEEE
ZISHU HE ¹, Member, IEEE

University of Electronic Science and Technology of China, Chengdu, China

BIN LIAO ¹, Senior Member, IEEE
Shenzhen University, Shenzhen, China

XUEPAN ZHANG ²
Qian Xuesen Laboratory of Space Technology, Beijing, China

WEILAI PENG ¹
University of Electronic Science and Technology of China, Chengdu, China

This paper presents a novel robust quasi-adaptive beamforming (RQAB) scheme against direction-of-arrival (DOA) mismatch. Unlike existing robust adaptive beamforming (RAB) methods, the proposed approach obtains the ultimate beamformer weight vector in a quiescent manner, nevertheless, it possesses the remarkable ability of interference rejection and desired signal reception. In this method, a two-step procedure is devised to design the quasi-adaptive weight vector. More specifically, the conventional sample matrix inversion (SMI) beamformer is first applied to find out all notch angles outside the region of interest (ROI) where the desired signal comes with a high probability. It is shown that these notch angles contain the DOAs of interferences. Then, a multipoint accurate array response control (MA²RC) algorithm is utilized to synthesize a beampattern with the

Manuscript received April 21, 2017; revised August 27, 2017; released for publication November 4, 2017. Date of publication November 22, 2017; date of current version June 7, 2018.

DOI No. 10.1109/TAES.2017.2776678

Refereeing of this contribution was handled by H. Mir.

This work was supported in part by the National Nature Science Foundation of China under Grant 61671139, Grant 61771316, and Grant 61701499, in part by the Foundation of the Department of Education of Guangdong Province under Grant 2016KTSCX125, and in part by the Nature Science Foundation of Guangdong Province under Grant 2017A030313341.

Authors' addresses: Xuejing Zhang, Z. He, and W. Peng are with the University of Electronic Science and Technology of China, Chengdu 611731, China, E-mail: (xjzhang7@163.com; zshe@uestc.edu.cn; lestinpw@163.com); B. Liao is with the College of Information Engineering, Shenzhen University, Shenzhen 518060, China, E-mail: (binliao@szu.edu.cn); Xuepan Zhang is with Qian Xuesen Laboratory of Space Technology, Beijing 100094, China, E-mail: (zhangxuepan@qxslab.cn). (*Corresponding author: Xuejing Zhang.*)

0018-9251 © 2017 IEEE

same sidelobe notch levels as the SMI, and nearly constant response over the ROI. Contrary to conventional approaches that are vulnerable to the contamination of the training data by the desired signal, our proposed approach exhibits outstanding performance under this common scenario. Moreover, besides the DOA mismatch, the proposed approach is also insensitive to the SNR, number of snapshots and mismatch angle. Additionally, different from many optimization-based RAB methods, the proposed RQAB approach offers an analytical expression of the beamformer weight vector and, hence, is computationally attractive. Typical simulation examples are provided to demonstrate the superiority of the RQAB scheme.

I. INTRODUCTION

Adaptive beamforming is one of important techniques in array signal processing and has been widely applied to radar, remote sensing, and wireless communications [1]–[6]. Briefly speaking, adaptive beamforming is a versatile and powerful approach to receiving signals of interest in the presence of interferences and noise. One of the most classical adaptive beamforming methods was developed by Capon [7], upon the assumption that the desired signal is absent from the training data and the knowledge of the direction-of-arrival (DOA) of the desired signal is available. Under this condition, the Capon beamformer enjoys both high resolution and good interference suppression [8]. However, it is known that this approach is quite sensitive to array imperfections, such as the DOA mismatch, imperfect array calibration, distorted antenna shape, and so on [9]–[11]. In view of this, robust adaptive beamforming (RAB) techniques, which improve the capability of countering errors, are of great importance.

During the past decades, numerous RAB approaches have been proposed. For instance, the linearly constrained minimum variance (LCMV) beamformer [12] is able to provide robustness against uncertainty in the look direction. Alternatively, diagonal loading (DL) techniques [13], [14] have been applied to the conventional Capon beamformer. However, the performance of the DL approach essentially depends on the loading factor which is quite challenging to select. A covariance matrix taper (CMT) technique, which can be regarded as a generalization of DL, is employed in [15] to enhance the robustness of adaptive beamformer. Nevertheless, the design of tapering matrix needs further investigation. The eigenspace-based beamformer developed in [16] involves projection of the presumed steering vector into the observed signal-plus-interference subspace, and thus is capable of overcoming the problem of array parameter perturbation. However, it cannot offer satisfactory performance when the signal-to-noise-ratio (SNR) is not sufficiently high and the number of signal plus interferences is relatively large. A robust Capon beamformer (RCB) is devised in [17] and [18] by extending the Capon beamformer to scenarios with steering vector uncertainties. This method belongs to the class of diagonal loading approaches. However, the loading level depends on the norm bound of the uncertainty set, which is usually unavailable in practice.

To overcome the performance degradation in the presence of large steering vector mismatches, an iterative robust Capon beamformer (IRCB) method with adaptive

uncertainty level is devised in [19]. This approach iteratively estimates the actual steering vector based on the RCB method. At each iteration, the adaptive uncertainty algorithm self-adjusts the uncertainty sphere according to the estimated mismatch steering vector. In [20], a worst-case optimization approach that can also be interpreted as a diagonal loading approach was presented. An extension of this approach was then developed in [21], where the parameters of the uncertainty region in terms of the beamformer outage probability is explicitly quantified. These two methods are based on convex optimization, so they do not provide a closed-form solution and cannot have simple online implementations. In [22], the RAB problem is tackled through steering vector estimation (SVE). This method only requires imprecise knowledge of the array geometry and angular sector. With a low-complexity shrinkage-based mismatch estimation (LOCSME) algorithm, another SVE-based RAB method is proposed in [23]. A covariance matrix reconstruction (CMR) based RAB method using an annulus uncertainty set to constrain the steering vectors of the interferences is developed in [24]. This method is robust against unknown arbitrary-type mismatches, but suffers from a large amount of calculation because of solving the integral involved.

Recently, Krylov-subspace algorithms have been widely applied to RAB. For instance, a family of low-complexity robust adaptive beamformers for large arrays in snapshot deficient scenarios have been devised in [25]. These approaches, which combine the Krylov-subspace-based dimensionality reduction method and robust Capon beamforming method, are capable of providing excellent robustness against both steering vector mismatch and rank overdetermination. In [26], the conjugate gradient (CG) algorithm, which originates from Krylov subspace methods, is adopted for RAB. More precisely, a diagonal loading CG beamformer and a reduced-rank CG beamformer have been developed. These two robust beamformers are more suitable than other RAB techniques to be implemented in field programmable gate array (FPGA) for real-time processing. In addition, a series of orthogonal Krylov subspace projection mismatch estimation (OKSPME) based low complexity RAB algorithms have been proposed in [27].

In particular, many efforts have been devoted to the problem of robust beamforming against DOA mismatch, which is also the focus of this work. To tackle this problem, magnitude response constraints have been introduced to design beamformers with a specified beamwidth and response ripple in [28] and [29]. An iterative second-order cone programming (SOCP) based beamformer with magnitude response constraints has been developed in [30] by solving a sequence of convex subproblems. A beamforming framework based on the usage of a set of beampattern shaping constraints is proposed in [31]. It achieves adaptive interference rejection and robustness against large DOA mismatch. Xu *et al.* devised a robust LCMV beamforming approach by utilizing response vector optimization in [32]. This method finds the optimal response vector in lieu of the all-one response vector in the traditional LCMV beamformer. A robust beamforming approach that can accurately

control the array main beam has been developed recently in [33]. For a more comprehensive review of the RAB methods, the interested reader is referred to [34].

It is noteworthy that in general the aforementioned methods are vulnerable to the presence of desired signal in the training data, due to the fact that the desired signal would be suppressed to some extent during the rejection of the interferences. Hence, they cannot offer satisfactory performance especially at high SNRs and when DOA mismatch exists. Moreover, most of the methods mentioned above determine the beamformer weight vector through the convex optimization techniques, and therefore, cannot provide analytical solutions in general. In light of these shortcomings, a new beamformer, which is robust against DOA mismatch, insensitive to the presence of desired signal in the training data, and able to offer an analytical expression of the beamformer weight vector, is designed in this paper.

To combat DOA mismatch, it is desirable to maintain the response of the beamformer nearly constant over the region of interest (ROI) where the desired signal comes with a high probability [28]–[33]. Therefore, the proposed beamformer shall be designed under this consideration. More importantly, in order to prevent the desired signal from self-nulling, the beamformer weight vector is designed in a quasi-adaptive manner, i.e., jointly using adaptive (data-dependent) and fixed (data-independent) beamforming techniques, rather than merely depending upon the training data contaminated by the desired signal. This leads to the so-called robust quasi-adaptive beamformer (RQAB). In this approach, a two-step procedure is carried out. More specifically, all possible directions of interferences are first determined according to the beampattern of the conventional sample matrix inversion (SMI) beamformer. On this basis, the multipoint accurate array response control (MA²RC) algorithm [35] is applied to obtain the beamformer weight vector, which can be analytically expressed. Simulation results show that the proposed RQAB approach results in a beampattern as expected and achieves higher output signal-to-interference-plus-noise ratio (SINR) than those of existing methods.

The paper is organized as follows. In Section II, the problem of robust adaptive beamforming is formulated and the MA²RC algorithm is briefly introduced. The proposed RQAB method is specified in Section III. In Section IV, numerical examples are conducted to demonstrate the excellent performance and effectiveness of the proposed method. Conclusions are drawn in Section V.

II. PRELIMINARIES

A. Robust Adaptive Beamforming Formulation

Let us consider a array with N isotropic sensor elements. Without loss of generality and for the sake of clarity, we focus on herein the problem of one-dimensional scenario. The steering vector in direction θ can be written as

$$\mathbf{a}(\theta) = [e^{-j\omega\tau_1(\theta)}, e^{-j\omega\tau_2(\theta)}, \dots, e^{-j\omega\tau_N(\theta)}]^T \quad (1)$$

where $(\cdot)^T$ stands for transpose, $j = \sqrt{-1}$ denotes the imaginary unit, $\tau_n(\theta)$ represents the time-delay between the n th

element and the reference point, and ω denotes the operating frequency. The output of a narrowband beamformer is given by

$$y(t) = \mathbf{w}^H \mathbf{x}(t) \quad (2)$$

where $(\cdot)^H$ stands for the conjugate transpose, t is the time index, \mathbf{w} is the $N \times 1$ complex vector of beamformer weights. $\mathbf{x}(t)$ in (2) is the array observation vector which is composed of the components of signal, interference and noise, and is expressed as

$$\mathbf{x}(t) = \mathbf{a}(\theta_0)s(t) + \mathbf{i}(t) + \mathbf{n}(t) \quad (3)$$

where θ_0 is the nominal DOA of the desired signal, $s(t)$ is the signal waveform, $\mathbf{i}(t)$ and $\mathbf{n}(t)$ denote the components of interference and noise, respectively. The optimal weight vector \mathbf{w}_{opt} , which maximizes the SINR, is given by

$$\mathbf{w}_{\text{opt}} = \alpha \mathbf{R}_{n+i}^{-1} \mathbf{a}(\theta_0) \quad (4)$$

where α is the normalization factor that does not affect the output SINR, $\mathbf{a}(\theta_0)$ is the signal steering vector, and \mathbf{R}_{n+i} denotes the $N \times N$ noise-plus-interference covariance matrix as

$$\mathbf{R}_{n+i} = \text{E} \{ (\mathbf{i}(t) + \mathbf{n}(t)) (\mathbf{i}(t) + \mathbf{n}(t))^H \}. \quad (5)$$

In practical applications, \mathbf{R}_{n+i} is not exactly available. Usually, the following sample covariance matrix is used:

$$\hat{\mathbf{R}}_x = \frac{1}{L} \sum_{l=1}^L \mathbf{x}(l) \mathbf{x}^H(l) \quad (6)$$

where L is the number of training snapshots. In this case, the beamformer weight vector, which is commonly referred to as the SMI, is given by

$$\mathbf{w}_{\text{SMI}} = \hat{\mathbf{R}}_x^{-1} \mathbf{a}(\theta_0). \quad (7)$$

It is known that in the case of signal-free training samples, the use of weight vector (7) provides rapid convergence of the output SINR to its optimal value. However, this is no longer true if the training snapshots are contaminated by the signal component. Another shortcoming of the SMI algorithm is that it cannot provide sufficient robustness against DOA mismatch, which will cause a substantial performance degradation when the presumed DOA (i.e., θ_0) of the desired signal is deviated from the actual one. In this mismatch case, the actual steering vector $\mathbf{a}(\tilde{\theta}_0)$ can be denoted as

$$\mathbf{a}(\tilde{\theta}_0) = \mathbf{a}(\theta_0 + \Delta\theta) \quad (8)$$

where $\tilde{\theta}_0 = \theta_0 + \Delta\theta$ is the actual direction of signal, $\Delta\theta$ stands for the direction mismatch which is unknown or imprecisely known in practice. As a result, the beamformer described in (7) tends to interpret the desired signal as interference and attempts to suppress it by means of adaptive nulling rather than maintaining undistorted response toward $\tilde{\theta}_0$. Therefore, numerous robust beamforming algorithms have been developed to improve its performance, see, e.g., [28]–[33] and related references therein.

B. MA²RC Algorithm

The MA²RC algorithm is a pattern synthesis approach to accurately controlling the response levels at multiple directions [35]. More precisely, this algorithm simultaneously control the responses at M directions $\theta_1, \dots, \theta_M$, by designing a weight vector \mathbf{w} satisfying

$$L(\theta_m, \theta_0) = \frac{|\mathbf{w}^H \mathbf{a}(\theta_m)|^2}{|\mathbf{w}^H \mathbf{a}(\theta_0)|^2} = \rho_m \quad \forall m \in \{1, \dots, M\} \quad (9)$$

where ρ_m is the desired response level at θ_m . In order to solve (9), a series of weight vectors $\tilde{\mathbf{w}}(\theta_1), \dots, \tilde{\mathbf{w}}(\theta_M)$ are first obtained as

$$\tilde{\mathbf{w}}(\theta_m) = \mathbf{a}(\theta_0) + \mu_m \mathbf{a}(\theta_m), \quad m = 1, \dots, M \quad (10)$$

where μ_m is determined by the A²RC algorithm [36] under the following condition as

$$\frac{|\tilde{\mathbf{w}}^H(\theta_m) \mathbf{a}(\theta_m)|^2}{|\tilde{\mathbf{w}}^H(\theta_m) \mathbf{a}(\theta_0)|^2} = \rho_m. \quad (11)$$

To proceed, let us assume $\theta_m \neq \theta_0$ and define $\mathbf{H}(\theta_m)$ as

$$\mathbf{H}(\theta_m) \triangleq [\mathbf{U}_2(\theta_m) \tilde{\mathbf{w}}(\theta_m)] \quad (12)$$

where $\mathbf{U}_2(\theta_m)$ spans the left null space of $[\mathbf{a}(\theta_0) \mathbf{a}(\theta_m)]$. More exactly, suppose that the singular value decomposition (SVD) of $[\mathbf{a}(\theta_0) \mathbf{a}(\theta_m)]$ is denoted as

$$[\mathbf{a}(\theta_0) \mathbf{a}(\theta_m)] = \mathbf{U}(\theta_m) \Sigma(\theta_m) \mathbf{V}^H(\theta_m) \quad (13)$$

where $\mathbf{U}(\theta_m)$ and $\mathbf{V}(\theta_m)$ include the left-singular vectors and right-singular vectors, respectively, and $\Sigma(\theta_m)$ includes the singular values. $\mathbf{U}_2(\theta_m)$ can thus be obtained by partitioning $\mathbf{U}(\theta_m)$ as

$$\mathbf{U}(\theta_m) = \underbrace{[\mathbf{u}_1 \ \mathbf{u}_2]}_{\mathbf{U}_1(\theta_m)} \underbrace{[\mathbf{u}_3 \ \dots \ \mathbf{u}_N]}_{\mathbf{U}_2(\theta_m)}. \quad (14)$$

Moreover, from (10), (13) and (14), it is known that

$$\mathbf{a}(\theta_0) \in \mathcal{R}^\perp(\mathbf{U}_2(\theta_m)) \quad (15)$$

$$\tilde{\mathbf{w}}(\theta_m) \in \mathcal{R}^\perp(\mathbf{U}_2(\theta_m)) \quad (16)$$

where $\mathcal{R}(\cdot)$ returns the column space of a matrix, $(\cdot)^\perp$ gives the orthogonal complement of a subspace. With the above notations, a closed-form expression of the weight vector \mathbf{w} satisfy (9) is finally obtained as [35]

$$\mathbf{w} = c \mathbf{H}(\theta_1) \begin{bmatrix} -\mathbf{F}^\dagger \mathbf{q} + \mathbf{f}_n \\ 1 \end{bmatrix}, \quad c \neq 0 \quad \forall \mathbf{f}_n \in \mathcal{N}(\mathbf{F}) \quad (17)$$

where $\mathcal{N}(\cdot)$ represents the null space, \dagger denotes the pseudo-inverse of a matrix, \mathbf{F} and \mathbf{q} are, respectively, given by

$$\mathbf{F}(\theta_1, \theta_2, \dots, \theta_M) = \begin{pmatrix} [\mathbf{I} - \mathbf{H}(\theta_2) \mathbf{H}^\dagger(\theta_2)] \mathbf{U}_2(\theta_1) \\ [\mathbf{I} - \mathbf{H}(\theta_3) \mathbf{H}^\dagger(\theta_3)] \mathbf{U}_2(\theta_1) \\ \vdots \\ [\mathbf{I} - \mathbf{H}(\theta_M) \mathbf{H}^\dagger(\theta_M)] \mathbf{U}_2(\theta_1) \end{pmatrix} \quad (18)$$

and

$$\mathbf{q}(\theta_1, \theta_2, \dots, \theta_M) = \begin{pmatrix} [\mathbf{I} - \mathbf{H}(\theta_2)\mathbf{H}^\dagger(\theta_2)] \bar{\mathbf{w}}(\theta_1) \\ [\mathbf{I} - \mathbf{H}(\theta_3)\mathbf{H}^\dagger(\theta_3)] \bar{\mathbf{w}}(\theta_1) \\ \vdots \\ [\mathbf{I} - \mathbf{H}(\theta_M)\mathbf{H}^\dagger(\theta_M)] \bar{\mathbf{w}}(\theta_1) \end{pmatrix}. \quad (19)$$

Note that the input variables of \mathbf{F} and \mathbf{q} , i.e., $\theta_1, \dots, \theta_M$, have been omitted in (17) for notational simplicity. The expression of \mathbf{w} in (17) gives the solution to (9) and plays an important role in the proposed RQAB algorithm.

III. ROBUST QUASI-ADAPTIVE BEAMFORMING

As mentioned earlier, the training data is usually contaminated by the desired component, thus deteriorating the performance of conventional beamformers, especially when the array suffers DOA mismatch. This motivates us to introduce a novel robust quasi-adaptive beamforming scheme in the sequel. From the interference rejection ability of the SMI beamformer, it is found that all possible angles of the interferences can be collected according to the beampattern of SMI. On this basis, the MA²RC algorithm can be adopted to synthesize a quasi-adaptive pattern with the same normalized response levels as SMI at all potential angles of the interferences, meanwhile, achieve a flat response in the ROI.

A. Analysis of SMI Beamformer in Interference Suppression

When training samples are contaminated by desired signal, the array covariance matrix \mathbf{R}_x can be expressed as

$$\mathbf{R}_x = \sigma_s^2 \mathbf{a}(\tilde{\theta}_0) \mathbf{a}^H(\tilde{\theta}_0) + \sum_{q=1}^Q \sigma_q^2 \mathbf{a}(\theta_q) \mathbf{a}^H(\theta_q) + \sigma_n^2 \mathbf{I} \quad (20)$$

where $\tilde{\theta}_0 = \theta_0 + \Delta\theta$ is the actual direction of signal, and θ_0 denotes the presumed one, Q denotes the total number of interference, σ_s^2 , σ_n^2 , and σ_q^2 stand for the signal power, noise power, and power of the q th interference, respectively. Let the eigendecomposition of \mathbf{R}_x be

$$\mathbf{R}_x = \sum_{q=1}^N \lambda_q \mathbf{v}_q \mathbf{v}_q^H \quad (21)$$

where λ_q and \mathbf{v}_q ($q = 1, \dots, N$) stand for the eigenvalues and the corresponding eigenvectors of \mathbf{R}_x , respectively, the eigenvalues are arranged in descending order. Thus, the corresponding weight vector, which is a mismatched version of \mathbf{w}_{opt} in (4), is given by

$$\mathbf{w}_e = \mathbf{R}_x^{-1} \mathbf{a}(\theta_0) = \sum_{q=1}^N \frac{\mathbf{v}_q^H \mathbf{a}(\theta_0)}{\lambda_q} \mathbf{v}_q. \quad (22)$$

Let us first consider the common case that the interferences are sufficiently stronger than powers of both signal and noise. In this case, we have

$$\lambda_1 \geq \dots \geq \lambda_Q \gg \lambda_{Q+1} \geq \dots \geq \lambda_N \quad (23)$$

and \mathbf{w}_e can be approximated as

$$\mathbf{w}_e \approx \sum_{q=Q+1}^N \gamma_q \mathbf{v}_q \in \mathcal{R}^\perp([\mathbf{a}(\theta_1), \dots, \mathbf{a}(\theta_q)]) \quad (24)$$

where $\gamma_q \triangleq \mathbf{v}_q^H \mathbf{a}(\theta_0) / \lambda_q$. The other common scenario is that the powers of interferences and desired signal are comparable but much stronger than that of the noise. Therefore, one can similarly obtain that

$$\lambda_1 \geq \dots \geq \lambda_Q \geq \lambda_{Q+1} \gg \lambda_{Q+2} \geq \dots \geq \lambda_N. \quad (25)$$

and accordingly, we have

$$\begin{aligned} \mathbf{w}_e &\approx \sum_{q=Q+2}^N \gamma_q \mathbf{v}_q \in \mathcal{R}^\perp([\mathbf{a}(\tilde{\theta}_0), \mathbf{a}(\theta_1), \dots, \mathbf{a}(\theta_q)]) \\ &\subseteq \mathcal{R}^\perp([\mathbf{a}(\theta_1), \dots, \mathbf{a}(\theta_q)]). \end{aligned} \quad (26)$$

From (24) and (26), it is noticed that \mathbf{w}_e is approximately perpendicular to the interference steering vectors in either case. In other words, the beampattern includes notches at the directions where the interferences come from. Furthermore, it is known from (26) that \mathbf{w}_e becomes approximately perpendicular to the actual signal steering vector $\mathbf{a}(\tilde{\theta}_0)$. As a result, the resulting \mathbf{w}_e will null the desired signal and accordingly degrade the performance of beamformer especially in a high SNR scenario.

Based on the above observations, we propose to design a quasi-adaptive pattern to improve the robustness of the conventional SMI beamformer. Specifically, this quasi-adaptive pattern produces the same response levels as the SMI method at the directions where interferences exist. On the other hand, the mainbeam response of the synthesized pattern should be nearly constant over the ROI to prevent the desired signal from being suppressed. Furthermore, to make the beamformer insensitive to the contamination of the training data by the desired signal, data-independent beamforming is incorporated into the design procedure.

B. Determination of Potential Directions of Interferences

In the previous section, the basic concept of the quasi-adaptive beamformer is briefly introduced. Prior to giving the detailed designing procedure of quasi-adaptive weight vector, we first propose a simple but effective strategy to determine all potential directions where interferences may exist and, meanwhile, obtain the corresponding response levels at those directions. Let the normalized response of \mathbf{w}_{SMI} be

$$L_e(\theta) = \frac{|\mathbf{w}_{\text{SMI}}^H \mathbf{a}(\theta)|^2}{\max\{|\mathbf{w}_{\text{SMI}}^H \mathbf{a}(\theta)|^2\}} \quad (27)$$

then any direction where $L_e(\theta)$ shapes a notch is probably the DOA of an interference. Therefore, we can obtain the set Θ_S that contains all potential directions of interferences by finding out all sidelobe notches of $L_e(\theta)$ as

$$\begin{aligned} \Theta_S &= \left\{ \theta \mid L_e(\theta) < \min\{L_e(\theta - \xi), L_e(\theta + \xi)\}, \theta \in \Omega_S \right\} \\ &= \{\check{\theta}_1, \check{\theta}_2, \dots, \check{\theta}_D\} \end{aligned} \quad (28)$$

where Ω_S denotes the sidelobe region, ξ is a small positive constant, and D is the number of notches in the sidelobe region. Since $L_e(\theta)$ is able to suppress interferences satisfactorily, we choose to set the desired levels of the expected quasi-adaptive beampattern $L(\theta, \theta_0)$ at the potential directions of interference, as their corresponding outputs at $L_e(\theta)$, i.e.,

$$L(\theta, \theta_0) = L_e(\theta) \quad \forall \theta \in \Theta_S. \quad (29)$$

In the mainlobe region, i.e., ROI, a nearly constant response is desirable for improving the robustness of the beamformer against the pointing errors. According to the LCMV approach [12], we can restrict the response levels at several discrete directions in the ROI. The set describing those discrete directions can be expressed as

$$\Theta_M = \{\tilde{\theta}_1, \tilde{\theta}_2, \dots, \tilde{\theta}_M\}, \quad \tilde{\theta}_m \in \Omega_M \quad (30)$$

where Ω_M stands for the mainlobe region, M is the number of discretizations in mainlobe region.

C. Designing Quasi-Adaptive Beamformer via MA²RC

Once the potential directions of interferences have been determined, the problem of designing a robust quasi-adaptive beamformer against DOA mismatch can be expressed as

$$\text{find } \mathbf{w} \quad (31a)$$

$$\text{subject to } L(\theta, \theta_0) = 1, \text{ for } \theta \in \Theta_M \quad (31b)$$

$$L(\theta, \theta_0) = L_e(\theta), \text{ for } \theta \in \Theta_S. \quad (31c)$$

However, the solution to (31) does not guarantee an optimal weight vector which maximizes the output SINR defined as $(\sigma_s^2 |\mathbf{w}^H \mathbf{a}(\tilde{\theta}_0)|) / (\mathbf{w}^H \mathbf{R}_{i+n} \mathbf{w})$. Therefore, the optimal weight vector should be obtained by solving the following problem

$$\max_{\mathbf{w}} \frac{\sigma_s^2 |\mathbf{w}^H \mathbf{a}(\tilde{\theta}_0)|}{\mathbf{w}^H \mathbf{R}_{i+n} \mathbf{w}} \quad (32a)$$

$$\text{subject to } L(\theta, \theta_0) = 1, \text{ for } \theta \in \Theta_M \quad (32b)$$

$$L(\theta, \theta_0) = L_e(\theta), \text{ for } \theta \in \Theta_S. \quad (32c)$$

To proceed, we rewrite the SINR, i.e., the objective function in the above optimization problem as

$$\begin{aligned} \frac{\sigma_s^2 |\mathbf{w}^H \mathbf{a}(\tilde{\theta}_0)|}{\mathbf{w}^H \mathbf{R}_{i+n} \mathbf{w}} &= \frac{\sigma_s^2 |\mathbf{w}^H \mathbf{a}(\tilde{\theta}_0)|^2}{\sigma_n^2 \|\mathbf{w}\|_2^2 + \sum_{q=1}^Q \sigma_q^2 |\mathbf{w}^H \mathbf{a}(\theta_q)|^2} \\ &= \frac{\sigma_s^2}{\frac{\sigma_n^2 \|\mathbf{w}\|_2^2}{|\mathbf{w}^H \mathbf{a}(\tilde{\theta}_0)|^2} + \underbrace{\sum_{q=1}^Q \frac{\sigma_q^2 |\mathbf{w}^H \mathbf{a}(\theta_q)|^2}{|\mathbf{w}^H \mathbf{a}(\tilde{\theta}_0)|^2}}_{\text{const}}} \end{aligned} \quad (33)$$

where the term $\sum_{q=1}^Q \frac{\sigma_q^2 |\mathbf{w}^H \mathbf{a}(\theta_q)|^2}{|\mathbf{w}^H \mathbf{a}(\tilde{\theta}_0)|^2}$ is actually a constant under the conditions in (31). This is because $\tilde{\theta}_0$ and θ_0 are located in the mainlobe region and, hence, achieving the same response level (i.e., $|\mathbf{w}^H \mathbf{a}(\tilde{\theta}_0)|^2 = |\mathbf{w}^H \mathbf{a}(\theta_0)|^2$). On the other hand, we have $|\mathbf{w}^H \mathbf{a}(\theta_q)|^2 / |\mathbf{w}^H \mathbf{a}(\tilde{\theta}_0)|^2 =$

$|\mathbf{w}^H \mathbf{a}(\theta_q)|^2 / |\mathbf{w}^H \mathbf{a}(\theta_0)|^2 = L_e(\theta_q)$, $q = 1, \dots, Q$, $\theta_q \in \Theta_S$. Obviously, it can be inferred that $|\mathbf{w}^H \mathbf{a}(\theta_q)|^2 / |\mathbf{w}^H \mathbf{a}(\tilde{\theta}_0)|^2$ is a constant.

From the above analysis, it is readily known that the maximization of output SINR is equivalent to the minimization of $\|\mathbf{w}\|_2^2 / |\mathbf{w}^H \mathbf{a}(\theta_0)|^2$, i.e.,

$$\max \text{SINR} \Leftrightarrow \min \frac{\|\mathbf{w}\|_2^2}{|\mathbf{w}^H \mathbf{a}(\theta_0)|^2}. \quad (34)$$

As a result, the quasi-adaptive beamformer can be designed as

$$\min_{\mathbf{w}} \frac{\|\mathbf{w}\|_2^2}{|\mathbf{w}^H \mathbf{a}(\theta_0)|^2} \quad (35a)$$

$$\text{subject to } L(\theta, \theta_0) = 1, \text{ for } \theta \in \Theta_M \quad (35b)$$

$$L(\theta, \theta_0) = L_e(\theta), \text{ for } \theta \in \Theta_S. \quad (35c)$$

Combining the weight vector formulation of MA²RC [i.e., (17)], we can find out the optimal quasi-adaptive weight vector by solving the problem as

$$\min_{\mathbf{w}} \frac{\|\mathbf{w}\|_2^2}{|\mathbf{w}^H \mathbf{a}(\theta_0)|^2} \quad (36a)$$

$$\text{subject to } \mathbf{w} = c \mathbf{H}(\tilde{\theta}_1) \begin{bmatrix} (-\mathbf{F}^\dagger \mathbf{q} + \mathbf{f}_n)^\top & 1 \end{bmatrix}^\top \quad (36b)$$

$$\mathbf{f}_n \in \mathcal{N}(\mathbf{F}) \quad (36c)$$

$$c \neq 0 \quad (36d)$$

where \mathbf{F} and \mathbf{q} are now short for $\mathbf{F}(\tilde{\theta}_1, \dots, \tilde{\theta}_M, \check{\theta}_1, \dots, \check{\theta}_D)$ and $\mathbf{q}(\tilde{\theta}_1, \dots, \tilde{\theta}_M, \check{\theta}_1, \dots, \check{\theta}_D)$, respectively. According to (18) and (19), to determine \mathbf{F} and \mathbf{q} , the following matrices should be first obtained

$$\mathbf{H}(\tilde{\theta}_m) = [\mathbf{U}_2(\tilde{\theta}_m) \quad \bar{\mathbf{w}}(\tilde{\theta}_m)] \quad (37)$$

$$\mathbf{H}(\check{\theta}_d) = [\mathbf{U}_2(\check{\theta}_d) \quad \bar{\mathbf{w}}(\check{\theta}_d)] \quad (38)$$

where $\bar{\mathbf{w}}(\tilde{\theta}_m)$ is obtained with the A²RC approach by setting $L(\tilde{\theta}_m, \theta_0) = 1$, $\bar{\mathbf{w}}(\check{\theta}_d)$ can be similarly obtained by setting $L(\check{\theta}_d, \theta_0) = L_e(\check{\theta}_d)$.

D. Optimal Solution to the Quasi-Adaptive Weight Vector

An optimization problem with certain constraints [i.e., (36)] has been established in the previous section to maximize the output SINR. In this section, an analytical solution to this problem will be obtained to complete the proposed robust quasi-adaptive beamforming method.

For the sake of clarity, we first define

$$\mathbf{g} \triangleq -\mathbf{F}^\dagger \mathbf{q}. \quad (39)$$

It can be derived from (15) that $\mathbf{a}(\theta_0) \in \mathcal{R}^\perp(\mathbf{U}_2(\tilde{\theta}_1))$, i.e., $\mathbf{U}_2^H(\tilde{\theta}_1) \mathbf{a}(\theta_0) = \mathbf{0}$. Moreover, according to (36b), the weight vector \mathbf{w} satisfies

$$\begin{aligned} \mathbf{w}^H \mathbf{a}(\theta_0) &= c^* \begin{bmatrix} (\mathbf{g} + \mathbf{f}_n)^\top & 1 \end{bmatrix} \mathbf{H}^H(\tilde{\theta}_1) \mathbf{a}(\theta_0) \\ &= c^* \begin{bmatrix} (\mathbf{g} + \mathbf{f}_n)^\top & 1 \end{bmatrix} [\mathbf{U}_2(\tilde{\theta}_1) \quad \bar{\mathbf{w}}(\tilde{\theta}_1)]^H \mathbf{a}(\theta_0) \\ &= c^* \bar{\mathbf{w}}^H(\tilde{\theta}_1) \mathbf{a}(\theta_0). \end{aligned} \quad (40)$$

Algorithm 1: The RQAB Algorithm.

- 1: give $\mathbf{a}(\theta_0)$ and the set Θ_M
 - 2: estimate $\hat{\mathbf{R}}_x$ as (6), obtain \mathbf{w}_{SMI} as (7) and calculate $L_e(\theta)$ by using \mathbf{w}_{SMI}
 - 3: establish the set Θ_S by using (28) and store the values of $L_e(\theta)$ for $\theta \in \Theta_S$
 - 4: **for** $m = 1, 2, \dots, M$ **do**
 - 5: calculate μ_m by A²RC method [36] such that $L(\tilde{\theta}_m, \theta_0) = 1$
 - 6: obtain $\tilde{\mathbf{w}}(\tilde{\theta}_m) = \mathbf{a}(\theta_0) + \mu_m \mathbf{a}(\tilde{\theta}_m)$
 - 7: carry out SVD of $\mathbf{A}(\theta_0, \tilde{\theta}_m)$ to obtain $\mathbf{U}_2(\tilde{\theta}_m)$
 - 8: denote $\mathbf{H}(\tilde{\theta}_m) = [\mathbf{U}_2(\tilde{\theta}_m) \tilde{\mathbf{w}}(\tilde{\theta}_m)]$
 - 9: **end for**
 - 10: **for** $d = 1, 2, \dots, D$ **do**
 - 11: calculate μ_d by A²RC method [36] such that $L(\check{\theta}_d, \theta_0) = L_e(\check{\theta}_d)$
 - 12: obtain $\tilde{\mathbf{w}}(\check{\theta}_d) = \mathbf{a}(\theta_0) + \mu_d \mathbf{a}(\check{\theta}_d)$
 - 13: carry out SVD of $\mathbf{A}(\theta_0, \check{\theta}_d)$ to obtain $\mathbf{U}_2(\check{\theta}_d)$
 - 14: denote $\mathbf{H}(\check{\theta}_d) = [\mathbf{U}_2(\check{\theta}_d) \tilde{\mathbf{w}}(\check{\theta}_d)]$
 - 15: **end for**
 - 16: obtain $\mathbf{F}(\tilde{\theta}_1, \dots, \tilde{\theta}_M, \check{\theta}_1, \dots, \check{\theta}_D)$ as (18) and $\mathbf{q}(\check{\theta}_1, \dots, \check{\theta}_M, \check{\theta}_1, \dots, \check{\theta}_D)$ as (19), respectively
 - 17: output the optimal RQAB weight vector \mathbf{w}_* in (51)
-

In fact, given the weight vector $\tilde{\mathbf{w}}(\tilde{\theta}_1)$, $\tilde{\mathbf{w}}^H(\tilde{\theta}_1)\mathbf{a}(\theta_0)$ can be regarded as a constant. As a result, the objective function (36a) can be rewritten as

$$\begin{aligned} \frac{\|\mathbf{w}\|_2^2}{|\tilde{\mathbf{w}}^H \mathbf{a}(\theta_0)|^2} &= \frac{\|\mathbf{c} \mathbf{H}(\tilde{\theta}_1) [(\mathbf{g} + \mathbf{f}_n)^T \quad 1]^T\|_2^2}{|c^* \tilde{\mathbf{w}}^H(\tilde{\theta}_1) \mathbf{a}(\theta_0)|^2} \\ &= \frac{\|\mathbf{H}(\tilde{\theta}_1) [(\mathbf{g} + \mathbf{f}_n)^T \quad 1]^T\|_2^2}{|\tilde{\mathbf{w}}^H(\tilde{\theta}_1) \mathbf{a}(\theta_0)|^2}. \end{aligned} \quad (41)$$

Again, owing to the constant property of $|\tilde{\mathbf{w}}^H(\tilde{\theta}_1) \mathbf{a}(\theta_0)|^2$, the optimization problem of finding the optimal weight vector \mathbf{w} in (36) can be equivalently reformulated as finding the optimal \mathbf{f}_n to the problem as

$$\min_{\mathbf{f}_n} \|\mathbf{H}(\tilde{\theta}_1) [(\mathbf{g} + \mathbf{f}_n)^T \quad 1]^T\|_2^2 \quad (42a)$$

$$\text{subject to } \mathbf{f}_n \in \mathcal{N}(\mathbf{F}) \quad (42b)$$

and the optimal weight vector \mathbf{w} (denoted as \mathbf{w}_*) is thus given by

$$\mathbf{w}_* = c \mathbf{H}(\tilde{\theta}_1) [(\mathbf{g} + \mathbf{f}_{n,*})^T \quad 1]^T, \quad c \neq 0 \quad (43)$$

where $\mathbf{f}_{n,*}$ denotes the optimal solution to (42).

To proceed to derive the optimal solution to (42), it is of importance to notice from (16) that

$$\tilde{\mathbf{w}}(\tilde{\theta}_1) \in \mathcal{R}^\perp(\mathbf{U}_2(\tilde{\theta}_1)). \quad (44)$$

On this basis, we can obtain

$$\begin{aligned} &\|\mathbf{H}(\tilde{\theta}_1) [(\mathbf{g} + \mathbf{f}_n)^T \quad 1]^T\|_2^2 \\ &= \|\mathbf{U}_2(\tilde{\theta}_1) (\mathbf{g} + \mathbf{f}_n) + \tilde{\mathbf{w}}(\tilde{\theta}_1)\|_2^2 \\ &= \|\mathbf{U}_2(\tilde{\theta}_1) (\mathbf{g} + \mathbf{f}_n)\|_2^2 + \|\tilde{\mathbf{w}}(\tilde{\theta}_1)\|_2^2. \end{aligned} \quad (45)$$

Since $\|\tilde{\mathbf{w}}(\tilde{\theta}_1)\|_2^2$ is fixed, one gets

$$\mathbf{f}_{n,*} = \arg \min_{\mathbf{f}_n \in \mathcal{N}(\mathbf{F})} \|\mathbf{U}_2(\tilde{\theta}_1) (\mathbf{g} + \mathbf{f}_n)\|_2^2. \quad (46)$$

It should be noted that the columns of $\mathbf{U}_2(\tilde{\theta}_1)$ are perpendicular with each other, and we have

$$\mathbf{U}_2^H(\tilde{\theta}_1) \mathbf{U}_2(\tilde{\theta}_1) = \mathbf{I}. \quad (47)$$

More importantly, notice that \mathbf{g} and \mathbf{f}_n actually locate in two orthogonal subspaces [37]. Specifically, we have $\mathbf{g} \in \mathcal{R}(\mathbf{F}^H)$ and $\mathbf{f}_n \in \mathcal{N}(\mathbf{F}) = \mathcal{R}^\perp(\mathbf{F}^H)$, and

$$\mathbf{g}^H \mathbf{f}_n = 0. \quad (48)$$

From (47) and (48), it can be concluded that

$$\|\mathbf{U}_2(\tilde{\theta}_1) (\mathbf{g} + \mathbf{f}_n)\|_2^2 = \|\mathbf{g}\|_2^2 + \|\mathbf{f}_n\|_2^2. \quad (49)$$

Then, $\mathbf{f}_{n,*}$ in (46) can be given by

$$\mathbf{f}_{n,*} = \arg \min_{\mathbf{f}_n \in \mathcal{N}(\mathbf{F})} \|\mathbf{f}_n\|_2^2 = \mathbf{0}. \quad (50)$$

Recalling (43), the optimization problem (36) has been solved. Consequently, according to (39) and (50), we can analytically express the optimal quasi-adaptive weight vector \mathbf{w}_* as

$$\begin{aligned} \mathbf{w}_* &= c [\mathbf{U}_2(\tilde{\theta}_1) \quad \tilde{\mathbf{w}}(\tilde{\theta}_1)] [(\mathbf{g} + \mathbf{f}_{n,*})^T \quad 1]^T \\ &= c [-\mathbf{U}_2(\tilde{\theta}_1) \mathbf{F}^\dagger \mathbf{q} + \tilde{\mathbf{w}}(\tilde{\theta}_1)] \end{aligned} \quad (51)$$

where c can be any nonzero constant. Finally, the main steps of the proposed RQAB algorithm are summarized in Algorithm 1.

REMARK 1 As discussed in the previous work [35], at most $N - 1$ points can be simultaneously controlled by the MA²RC algorithm. Hence, the total number of discretizations in mainlobe region and selected potential directions of interferences should be no larger than $N - 1$, i.e., $D + M \leq N - 1$.

E. Computational Complexity

We now analyze the computational complexity of the proposed algorithm and compare it with several existing works. For brevity, we denote $\bar{M} = M + D$ in the sequel. Recalling (13) and (14), for a fixed m , $\mathbf{U}_2(\theta_m)$ can be actually obtained via Givens QR decomposition [38], which requires $(12N - 8)$ flops. Taking the flops of calculating $\tilde{\mathbf{w}}(\theta_m)$ [with a number of $(6N + 7)$] into account, the flops of computing $\mathbf{H}(\theta_m)$ is $(18N - 1)$. Since the columns of $\mathbf{U}_2(\theta_m)$ are orthogonal, it is known from [38] that $\mathbf{H}^\dagger(\theta_m)$ can be calculated by Householder QR algorithm, and that the computation of $\mathbf{I} - \mathbf{H}(\theta_m) \mathbf{H}^\dagger(\theta_m)$ requires $4(N + (N - 1)^2/3)$ flops once $\mathbf{H}(\theta_m)$ has been

TABLE I
Complexity Comparison

RAB algorithms	Flops
RCB [17]	$2N^3 + 11N^2$
Worse-case [20]	$O(N^{3.5})$
LOCSME [23]	$4N^3 + 3N^2 + 20N$
CMR [24]	$O(\max(SN^2, N^{3.5}))$
OKSPME [27]	$N^3 + (4k + 11)N^2 + (3k^2 + 5k + 20)N$
Proposed	$11(N - 2)^3/3 + 24N^2 - 33N + 7$

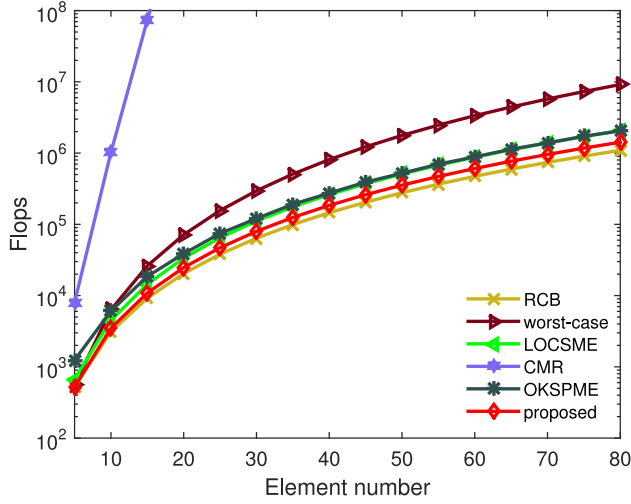


Fig. 1. Flops versus element number.

obtained. Combining the low-rank property of \mathbf{F} in (18) and \mathbf{q} in (19), the total flops of calculating \mathbf{w}_* in (51) is $(18N - 1)\bar{M} + 4(N + (N - 1)^2/3)(\bar{M} - 1) + (\bar{M} - 1)(N - 2)^2 + (\bar{M} - 1)^3/3 + N$. As a consequence, the worst-case (i.e., setting $\bar{M} = N - 1$) flops of our algorithm is $11(N - 2)^3/3 + 24N^2 - 33N + 7$.

Following the result shown in [27], we have listed the flops comparison of the proposed method and several existing ones in Table I. To have an intuitive perspective, we also depict the curves of flops versus element number in Fig. 1. In this test, we use $S = 10 \cdot 2^N$ for the CMR method [24]. Additionally, instead of setting k as a fixed number (see [27]), for the OKSPME method we set $k = \text{ceil}(N/2) + 1$, where $\text{ceil}(\cdot)$ rounds the input number toward positive infinity. From Fig. 1, it can be observed that the required flops of the proposed algorithm is a bit greater than that of RCB method, but less than the other four approaches.

IV. NUMERICAL RESULTS

In this section, representative simulations are carried out to demonstrate the effectiveness of the proposed robust quasi-adaptive beamforming scheme. We assume a nonuniformly spaced linear array of $N = 16$ omnidirectional sensors. The element positions are specified in Table II. There are one desired signal and two interfering sources. The interferences impinge on the array from the directions -60° and 25° , and the interference-to-noise ra-

TABLE II
Element Positions of the Nonuniform Linear Array

n	$x_n(\lambda)$	n	$x_n(\lambda)$	n	$x_n(\lambda)$	n	$x_n(\lambda)$
1	0.00	5	2.36	9	4.03	13	5.78
2	0.46	6	2.66	10	4.47	14	6.27
3	1.19	7	3.36	11	4.78	15	6.54
4	1.72	8	3.72	12	5.48	16	7.27

tios (INR) are 30 dB and 25 dB, respectively. It is assumed that there exists a mismatch between the actual direction of the desired signal and the presumed one. Unless otherwise specified, the actual direction of signal is $\tilde{\theta}_0 = 2^\circ$ while its presumed direction is $\theta_0 = 0^\circ$, the SNR is taken as 15 dB and the training snapshots is $L = 30$.

To obtain a pattern with nearly constant response in the ROI, we set $M = 2$ and prescribe two angles $\tilde{\theta}_1 = -1^\circ$ and $\tilde{\theta}_2 = 1^\circ$ when implementing the proposed RQAB method. The response levels at $\tilde{\theta}_1$ and $\tilde{\theta}_2$ are forced to 0 dB. The value of ξ in (28) is set as 0.5° .

For comparison purpose, the simulation results of the SMI beamformer, RCB beamformer [17], IRCB beamformer [19], worst-case optimization beamformer [20], RVO-LCMV method [32], SVE beamformer [22], and CMR beamformer [24] are presented as well. The norm bound ϵ in RCB is taken as 12.6442, which corresponds to a two-degrees mismatch. The values of ϵ in worst-case beamformer and CMR method are set as $0.5\sqrt{N}$ and 0.1, respectively. Additionally, to have a more comprehensive demonstration of the superiority of the proposed method, the performance of the SMI with DOA estimation is compared. For this beamformer, we first estimate the actual DOA of the desired signal according to the position of the beampattern null in the ROI. Thus, the SMI beamformer with DOA estimation can be expressed by replacing the presumed steering vector $\mathbf{a}(\theta_0)$ with the estimated one.

A. Comparison of the Beampatterns

In this section, the beampattern of the proposed RQAB method is compared with those of the existing approaches. As discussed previously, the SMI beamformer is first applied by using the mismatched steering vector, the corresponding beampattern is plotted in dashed line in Fig. 2. Obviously, it is seen that the SMI beamformer forms nulls at the directions of interferences. However, it suppresses the desired signal by forming a null at 2° as well.

On the basis of the SMI beamformer, the MA²RC approach is applied by first determining the directions of notches in the sidelobe region. In this example, there are $D = 11$ nulls in the sidelobe region. Meanwhile, the corresponding normalized response levels of notches are collected as the desired levels for MA²RC algorithm. Combining the two constrain directions $\tilde{\theta}_1$ and $\tilde{\theta}_2$ in the ROI, the MA²RC can thus be applied. The resulting beampattern with specific constraints is formed as shown in Fig. 2, where all constrained points are marked by asterisks to have a better illustration. From Fig. 2, it can be seen that in the sidelobe region, all the response levels at these

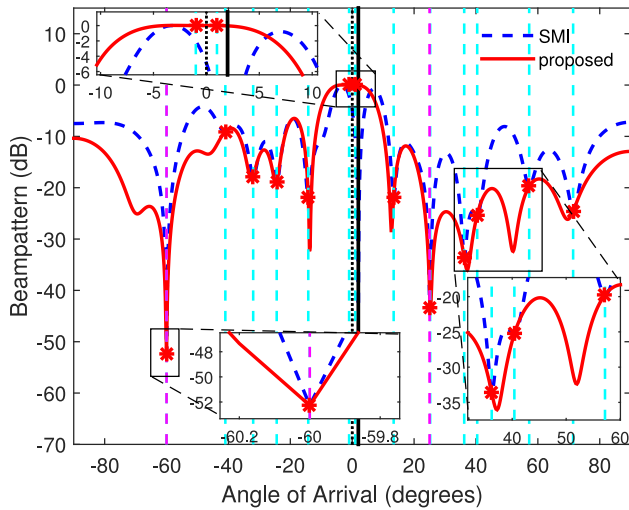


Fig. 2. Simulation results of SMI and RQAB.

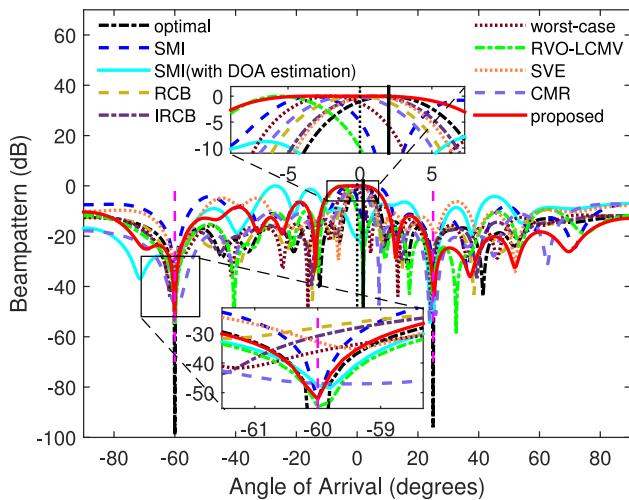


Fig. 3. Beampattern comparison.

asterisks remain unchanged, and the resultant response levels of the two constraint directions in ROI are equal to 0 dB as prescribed.

Fig. 3 compares the beampatterns of different methods. It can be clearly found that both RVO-LCMV beamformer and SMI beamformer with DOA estimation null the actual signal, mainly due to the insufficient snapshots. Note that an inaccurate estimation of DOA may also affect the performance of SMI beamformer with DOA estimation. Furthermore, it is observed (from the zoomed-in figure at -60°) that the RCB beamformer, IRCB beamformer, worst-case approach, and SVE method do not shape deep notches at the directions of interferences, thus cannot suppress interferences satisfactorily as the proposed RQAB algorithm.

B. Comparison of the Output SINRs

In this section, the output SINR is considered to further illustrate the performance of the proposed RQAB method. In particular, the output SINR versus SNR, number of snapshots and mismatch angle will be tested.

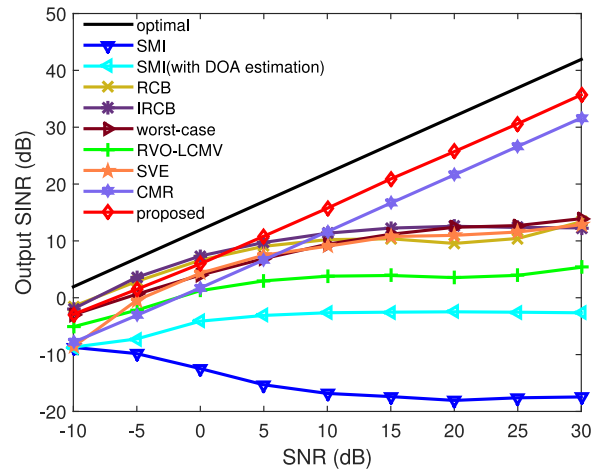


Fig. 4. SINR versus SNR for $L = 30$.

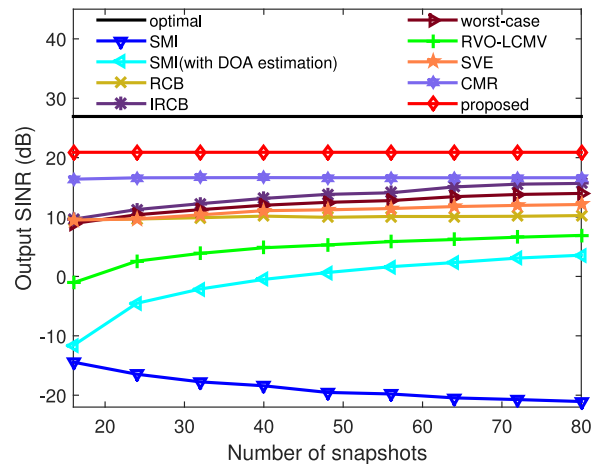


Fig. 5. SINR versus the number of snapshots for $\text{SNR} = 15$ dB.

1) *SINR Versus SNR*: First, the performance in terms of the SINR versus SNR is studied. We vary the SNR from -10 dB to 30 dB and depict the output SINRs of the beamformers tested in Fig. 4. It is seen that the proposed RQAB method substantially outperforms all other beamformers especially when the SNR is greater than 2 dB. In the lower SNR scenario, there is not much performance difference between the proposed RQAB method and other existing adaptive approaches.

2) *SINR Versus Number of Snapshots*: In this example, we study the beamforming performance (i.e., output SINR) versus the number of training snapshots that are utilized in estimating the array covariance matrix $\hat{\mathbf{R}}_x$. The input SNR is set to 15 dB. Simulation results are displayed in Fig. 5, from which it can be clearly seen that the proposed RQAB method outperforms the other beamformers tested.

3) *SINR Versus Mismatch Angle*: Now, we investigate the effect of mismatch angle [i.e., $\Delta\theta$ in (8)]. To this end, we set $\text{SNR} = 15$ and $L = 30$, and vary the mismatch angle from -3° to 3° . The resultant output SINR curves of different approaches are displayed in Fig. 6. It is seen that the proposed RQAB approach is quite robust against the DOA mismatch and the output SINR is nearly not affected

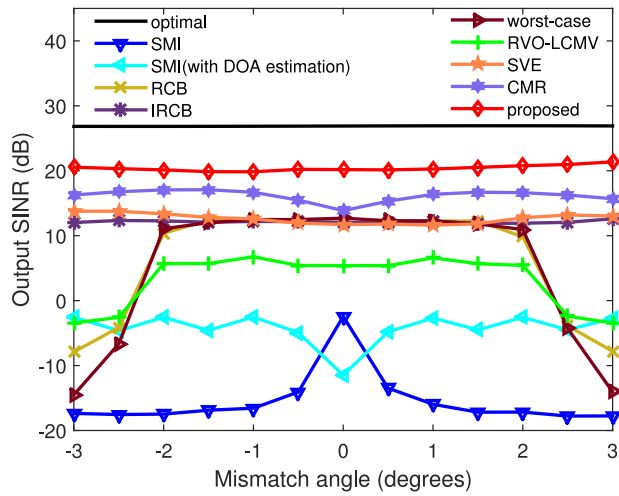


Fig. 6. SINR versus mismatch angle (SNR = 15 dB, $L = 30$).

by the mismatch level. Moreover, the proposed method outperforms all existing methods we tested. For the existing approaches, such as the SMI, RCB, worst-case, and RVO-LCMV algorithms, their performances tend to be worse when the mismatch angle is getting larger. Additionally, it is noticed that the SMI algorithm cannot provide satisfactory performance even in the absence of DOA mismatch, due to the insufficiency of training samples. Finally, the algorithm of SMI with DOA estimation performs relatively worse when there is no DOA mismatch because of the inaccuracy of DOA estimation.

V. CONCLUSION

In this paper, we have devised a novel robust quasi-adaptive beamforming (RQAB) algorithm against the DOA mismatch. This method results in a beam pattern with flat response in the mainlobe and suitable response levels at the angles of potential interferences. This pattern is designed by first finding out the angles of potential interferences from the response of the SMI beamformer. Then, the MA²RC algorithm is applied to adjust the responses in the mainlobe and sidelobe regions. To further improve the performance of the proposed method, the weight vector is optimized to maximize the output SINR. The RQAB method provides an analytical expression of the weight vector and requires less computation as compared with conventional approaches. Representative examples have been provided to validate the proposed method when the DOA is mismatched and training samples contain desired signal. Simulation results show that the devised approach is robust against the DOA mismatch. Moreover, it is insensitive to SNR, snapshots number and mismatch angle. As a future work, we shall extend the proposed quasi-adaptive approach to scenarios with arbitrary array errors other than DOA mismatch.

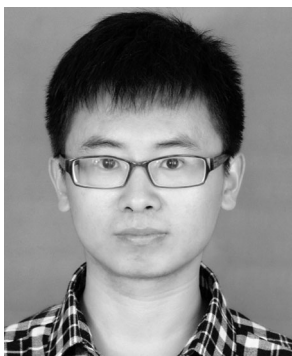
ACKNOWLEDGMENT

The authors would like to thank the anonymous reviewers for their valuable comments and suggestions.

REFERENCES

- [1] R. J. Mooloolous, *Phased Array Antenna Handbook*. Norwood, MA, USA: Artech House, 1994.
- [2] P. K. Bailleul, A new era in elemental digital beamforming for spaceborne communications phased arrays *Proc. IEEE*, vol. 104, no. 3, pp. 623–632, Mar. 2016.
- [3] F. Vanpoucke and M. Moonen, Systolic robust adaptive beamforming with an adjustable constraint *IEEE Trans. Aerosp. Electron. Syst.*, vol. 31, no. 2, pp. 658–669, Apr. 1995.
- [4] F. G. A. Neto, R. C. de Lamare, V. H. Nascimento, and Y. V. Zakharov, Adaptive reweighting homotopy algorithms applied to beamforming *IEEE Trans. Aerosp. Electron. Syst.*, vol. 51, no. 3, pp. 1902–1915, Jul. 2015.
- [5] B. Liao, S. C. Chan, and K. M. Tsui, Recursive steering vector estimation and adaptive beamforming under uncertainties *IEEE Trans. Aerosp. Electron. Syst.*, vol. 49, no. 1, pp. 489–501, Jan. 2013.
- [6] G. A. Fabrizio, A. B. Gershman, and M. D. Turley, Robust adaptive beamforming for HF surface wave over-the-horizon radar *IEEE Trans. Aerosp. Electron. Syst.*, vol. 40, no. 2, pp. 510–525, Apr. 2004.
- [7] J. Capon, High-resolution frequency-wavenumber spectrum analysis *Proc. IEEE*, vol. WC-57, no. 8, pp. 1408–1418, Aug. 1969.
- [8] I. S. Reed, J. D. Mallett, and L. E. Brennan, Rapid convergence rate in adaptive arrays *IEEE Trans. Aerosp. Electron. Syst.*, vol. AES-10, no. 6, pp. 853–863, Nov. 1974.
- [9] H. K. Van Trees, *Optimum Array Processing*. New York, NY, USA: Wiley, 2002.
- [10] J. Li and P. Stoica Eds, *Robust Adaptive Beamforming*. Hoboken, NJ, USA: Wiley, 2005.
- [11] L. Du, J. Li, and P. Stoica, Fully automatic computation of diagonal loading levels for robust adaptive beamforming *IEEE Trans. Aerosp. Electron. Syst.*, vol. 46, no. 1, pp. 449–458, Jan. 2010.
- [12] O. L. Frost, III, An algorithm for linearly constrained adaptive array processing *Proc. IEEE*, vol. WC-60, no. 8, pp. 926–935, Aug. 1972.
- [13] B. D. Carlson, Covariance matrix estimation errors and diagonal loading in adaptive arrays *IEEE Trans. Aerosp. Electron. Syst.*, vol. 24, no. 4, pp. 397–401, Jul. 1988.
- [14] H. Cox, R. M. Zeskind, and M. M. Owen, Robust adaptive beamforming *IEEE Trans. Acoust., Speech, Signal Process.*, vol. 35, no. 10, pp. 1365–1376, Oct. 1987.
- [15] J. R. Guerci and J. S. Bergin, Principal components, covariance matrix tapers, and the subspace leakage problem *IEEE Trans. Aerosp. Electron. Syst.*, vol. 38, no. 1, pp. 152–162, Jan. 2002.
- [16] D. D. Feldman and L. J. Griffiths, A projection approach for robust adaptive beamforming *IEEE Trans. Signal Process.*, vol. 42, no. 4, pp. 867–876, Apr. 1994.

- [17] J. Li, P. Stoica, and Z. Wang
On robust Capon beamforming and diagonal loading
IEEE Trans. Signal Process., vol. 51, no. 7, pp. 1702–1715, Jul. 2003.
- [18] P. Stoica, Z. Wang, and J. Li
Robust Capon beamforming
IEEE Signal Process. Lett., vol. 10, no. 6, pp. 172–175, Jun. 2003.
- [19] J. P. Lie, W. Ser, and C. M. S. See
Adaptive uncertainty based iterative robust Capon beamformer using steering vector mismatch estimation
IEEE Trans. Signal Process., vol. 59, no. 9, pp. 4483–4488, Sep. 2011.
- [20] S. A. Vorobyov, A. B. Gershman, and Z. Q. Luo
Robust adaptive beamforming using worst-case performance optimization: A solution to the signal mismatch problem
IEEE Trans. Signal Process., vol. 51, pp. 313–324, 2003.
- [21] S. A. Vorobyov, H. Chen, and A. B. Gershman
On the relationship between robust minimum variance beamformers with probabilistic and worst-case distortionless response constraints
IEEE Trans. Signal Process., vol. 56, no. 11, pp. 5719–5724, Nov. 2008.
- [22] A. Khabbazi-basmenj, S. A. Vorobyov, and A. Hassanien
Robust adaptive beamforming based on steering vector estimation with as little as possible prior information
IEEE Trans. Signal Process., vol. 60, no. 6, pp. 2974–2987, Jun. 2012.
- [23] H. Ruan and R. C. d. Lamare
Robust adaptive beamforming using a low-complexity shrinkage-based mismatch estimation algorithm
IEEE Signal Process. Lett., vol. 21, no. 1, pp. 60–64, Jan. 2014.
- [24] L. Huang, J. Zhang, X. Xu, and Z. Ye
Robust adaptive beamforming with a novel interference-plus-noise covariance matrix reconstruction method
IEEE Trans. Signal Process., vol. 63, no. 7, pp. 1643–1650, Apr. 2015.
- [25] S. D. Somasundaram, N. H. Parsons, L. Peng, and R. C. De Lamare
Reduced-dimension robust capon beamforming using Krylov-subspace techniques
IEEE Trans. Aerosp. Electron. Syst., vol. 51, no. 1, pp. 270–289, Jan. 2015.
- [26] M. Zhang, A. Zhang, and Q. Yang
Robust adaptive beamforming based on conjugate gradient algorithms
IEEE Trans. Signal Process., vol. 64, no. 22, pp. 6046–6057, Nov. 2016.
- [27] H. Ruan and R. C. d. Lamare
Robust adaptive beamforming based on low-rank and cross-correlation techniques
IEEE Trans. Signal Process., vol. 64, no. 15, pp. 3919–3932, Aug. 2016.
- [28] Z. L. Yu, M. H. Er, and W. Ser
A novel adaptive beamformer based on semidefinite programming (SDP) with magnitude response constraints
IEEE Trans. Antennas Propag., vol. 56, no. 5, pp. 1297–1307, May 2008.
- [29] Z. L. Yu, W. Ser, M. H. Er, Z. Gu, and Y. Li
Robust adaptive beamformers based on worst-case optimization and constraints on magnitude response
IEEE Trans. Signal Process., vol. 57, no. 7, pp. 2615–2628, Jul. 2009.
- [30] B. Liao, K. M. Tsui, and S. C. Chan
Robust beamforming with magnitude response constraints using iterative second-order cone programming
IEEE Trans. Antennas Propag., vol. 59, no. 9, pp. 3477–3482, Sep. 2011.
- [31] S. E. Nai, W. Ser, Z. L. Yu, and S. Rahardja
A robust adaptive beamforming framework with beam pattern shaping constraints
IEEE Trans. Antennas Propag., vol. 57, no. 7, pp. 2198–2203, Jul. 2009.
- [32] J. Xu, G. Liao, S. Zhu, and L. Huang
Response vector constrained robust LCMV beamforming based on semidefinite programming
IEEE Trans. Signal Process., vol. 63, no. 21, pp. 5720–5732, Nov. 2015.
- [33] B. Liao, C. Guo, L. Huang, Q. Li, and H. C. So
Robust adaptive beamforming with precise main beam control
IEEE Trans. Aerosp. Electron. Syst., vol. 53, no. 1, pp. 345–356, Feb. 2017.
- [34] A. B. Gershman, N. D. Sidiropoulos, S. ShahbazPanahi, M. Bengtsson, and B. Ottersten
Convex optimization-based beamforming
IEEE Signal Process. Mag., vol. 27, no. 3, pp. 62–75, May 2010.
- [35] X. Zhang, Z. He, B. Liao, X. Zhang, and W. Peng
Pattern synthesis with multipoint accurate array response control
IEEE Trans. Antennas Propag., vol. 65, no. 8, pp. 4075–4088, 2017.
- [36] X. Zhang, Z. He, B. Liao, X. Zhang, Z. Cheng, and Y. Lu
A²RC: An accurate array response control algorithm for pattern synthesis
IEEE Trans. Signal Process., vol. 65, pp. 1810–1824, Aug. 2017.
- [37] G. Strang
Linear Algebra and Its Applications, 4th ed. New York, NY, USA: Wellesley-Cambridge, 2005.
- [38] G. H. Golub and C. F. V. Loan
Matrix Computations. Baltimore, MD, USA: The Johns Hopkins Univ. Press, 1996.



Xuejing Zhang (S'17) was born in Hebei, China. He received the B.S. degree in electrical engineering from Huaqiao University, Xiamen, China, and the M.S. degree in signal and information processing from Xidian University, Xi'an, China, in 2011 and 2014, respectively. He is currently working toward the Ph.D. degree in signal and information processing with the Department of Electronic Engineering, University of Electronic Science and Technology of China, Chengdu, China.

Since November 2017, he has been a Visiting Student with the University of Delaware, Newark, DE, USA. From 2014 to 2015, he was a Research Engineer with Allwinner Inc., Zhuhai, China, where he was engaged in algorithmic research. His research interests include array signal processing, optimization theory, and machine learning.



Zishu He (M'11) was born in Chengdu, China, in 1962. He received the B.S., M.S., and Ph.D. degrees in signal and information processing from the University of Electronic Science and Technology of China (UESTC), Chengdu, China, in 1984, 1988, and 2000, respectively. He is currently a Professor in signal and information processing with the School of Electronic Engineering, UESTC.

His current research interests include array signal processing, digital beam forming, the theory on multiple-input multiple-output (MIMO) communication and MIMO radar, adaptive signal processing, and interference cancellation.



Bin Liao (S'09–M'13–SM'16) received the B.Eng. and M.Eng. degrees in electronic engineering from Xidian University, Xi'an, China, in 2006 and 2009, respectively, and the Ph.D. degree in electronic engineering from The University of Hong Kong, Hong Kong, in 2013.

From September 2013 to January 2014, he was a Research Assistant in the Department of Electrical and Electronic Engineering, The University of Hong Kong. From August 2016 to October 2016, he was a Research Scientist with the Department of Electrical and Electronic Engineering, The University of Hong Kong. He is currently an Associate Professor with the College of Information Engineering, Shenzhen University, Shenzhen, China. His research interests include sensor array processing, adaptive filtering, convex optimization, with applications to radar, navigation, and communications.

Dr. Liao was a recipient of the Best Paper Award at the 21st International Conference on Digital Signal Processing (2016 DSP) and 22nd International Conference on Digital Signal Processing (2017 DSP). He is an Associate Editor for *IET Signal Processing*, *Multidimensional Systems and Signal Processing* and IEEE ACCESS.



Xuepan Zhang was born in Hebei, China. He received the B.S. degree from Xidian University, Xi'an, China, in 2010, and the Ph.D. degree from the National Laboratory of Radar Signal Processing, Xi'an, China, in 2015, both in electrical engineering.

He is currently a Principal Investigator with Qian Xuesen Laboratory of Space Technology, Beijing, China. His research interests include synthetic aperture radar, ground moving target indication, and deep learning.



Weilai Peng received the B.Eng. degree in electronic engineering from the University of Electronic Science and Technology of China, Chengdu, China, in 2015, where he is currently working toward the Ph.D. degree in electronic engineering.

His research interests include array signal processing and MIMO radar.